JOURNAL OF THERMOPHYSICS AND HEAT TRANSFER
Vol. 10, No. 2, April–June 1996

Technical Notes

TECHNICAL NOTES are short manuscripts describing new developments or important results of a preliminary nature. These Notes cannot exceed 6 manuscript pages and 3 figures; a page of text may be substituted for a figure and vice versa. After informal review by the editors, they may be published within a few months of the date of receipt. Style requirements are the same as for regular contributions (see inside back cover).

Heat Removal from Tubes with Externally, Longitudinal Fins: Distributed and Lumped Models

Antonio Campo*
Idaho State University, Pocatello, Idaho 83209
and
Angela O. Nieckele†
Pontificia Universidade Catolica do Rio de Janeiro, 22453-900 Rio de Janeiro, Brazil

Nomenclature

c_{pi} = specific heat
D = tube diameter
h_e = local, external convective coefficient
$\bar{h}_i$ = mean, internal convective coefficient
k_i = thermal conductivity
$\dot{m}$ = mass flow rate
Pe_i = Peclet number, $\bar{w}D/\alpha_i$
R = tube radius
T, T_b = local, bulk temperature
T_0, T_∞ = inlet, ambient temperature
$\bar{w}$ = mean axial velocity
α_i = thermal diffusivity

Subscripts
e, i = external, internal fluid

Introduction

THE degree of heat transfer intensification in external, longitudinal finned tubes is sensitive to the number of fins in the array N, the external convective coefficient h_u, for the unfinned segment x_u, and the effective external convective coefficient h_f, for the finned segment x_f, respectively.

From a fundamental standpoint, this internal forced convective problem constitutes a three-dimensional thermal developing problem being subject to a boundary condition of the third kind, where the convective coefficient varies periodically along the periphery of the tube $h_e(\theta)$. To complement the three-dimensional numerical results, a one-dimensional approximate algebraic solution relying on a mean value of the external convective coefficient (independent of the angle θ) was carried out. Certainly, adoption of this mean value corresponds to a careful introduction of various spatial means of the external convective coefficient. Validation of these spatial means may be needed for purposes of exploring simplifications for the design of heat exchanger tubes.

Received Dec. 12, 1994; revision received Oct. 13, 1995; accepted for publication Oct. 13, 1995.

*Professor, Department of Nuclear Engineering. Member AIAA.
†Associate Professor, Department of Mechanical Engineering.

Problem Description

The inset of Fig. 1 depicts a circular, thin-walled tube fitted with an array of N external longitudinal fins. The internal fluid possesses 1) constant properties, 2) fully developed laminar velocity, and 3) a uniform temperature T_0 at the inlet $z = 0$. The effects of buoyancy and wall conduction are neglected in the analysis. The heat losses to the external fluid at T_∞ occur through a sequence of unfinned and finned portions of the tube.

The problem is characterized by the dimensionless variables

$$\phi = (T - T_0)/(T_\infty - T_0), \qquad Z = z/RPe_i, \qquad \eta = r/R \tag{1}$$

together with the dimensionless parameters

$$N, \quad X_f = x_f/D, \qquad Bi_f = h_f R/k_i, \qquad Bi_u = h_u R/k_i \tag{2}$$

Once the bulk temperature has been computed, the thermal quantity of importance to design engineers is the total heat transfer Q_T in a tube of length L. This may be calculated from a global energy balance

$$Q_T = \dot{m}c_{pi}[T_0 - T_b(L)] \tag{3}$$

that leads to a dimensionless heat transfer

$$\Omega_T = \frac{Q_T}{Q_{\max}} = \frac{Q_T}{\dot{m}c_{pi}(T_0 - T_\infty)} = \phi_b(\bar{L}) \tag{4}$$

in terms of $\phi_b(\bar{L})$, the bulk temperature, and $\bar{L} = L/RPe_i$, the axial position, both dimensionless.

Three-Dimensional Distributed Model

The dimensionless, three-dimensional energy conservation equation

$$(1 - \eta^2)\frac{\partial \phi}{\partial Z} = \frac{1}{\eta}\frac{\partial}{\partial \eta}\left(\eta \frac{\partial \phi}{\partial \eta}\right) + \frac{1}{\eta^2}\frac{\partial^2 \phi}{\partial \theta^2} \tag{5}$$

subjected to the boundary conditions

$$\phi = 0, \qquad Z = 0 \tag{6a}$$

$$\frac{\partial \phi}{\partial \eta} = 0, \qquad \eta = 0 \tag{6b}$$

$$-\frac{\partial \phi}{\partial \eta} = Bi_f(\phi - 1), \qquad \eta = 1, \quad \text{finned part} \tag{6c}$$

$$-\frac{\partial \phi}{\partial \eta} = Bi_u(\phi - 1), \qquad \eta = 1, \quad \text{unfinned part} \tag{6d}$$

$$\frac{\partial \phi}{\partial \theta} = 0, \qquad \frac{\pi}{N} \tag{6e}$$

$$\theta = 0, \qquad \frac{\pi}{N} \tag{6f}$$

was solved numerically by the finite volume method described by Patankar.[1] Accordingly, the resulting system of algebraic

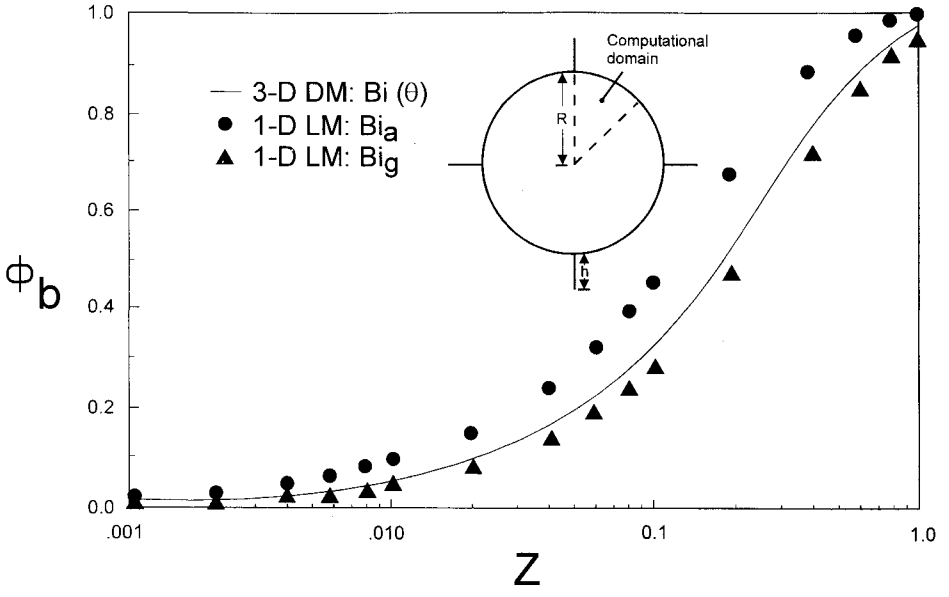

Fig. 1 Comparison of the bulk temperatures for $N = 4$.

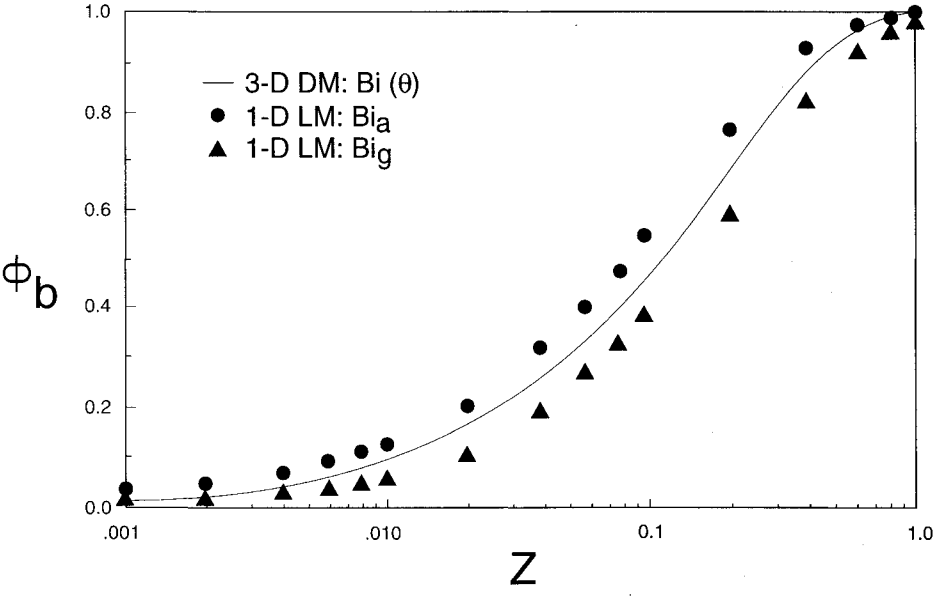

Fig. 2 Comparison of the bulk temperatures for $N = 16$.

equations was calculated by the line-by-line procedure of the tri-diagonal-matrix-algorithm (TDMA) coupled with the block correction algorithm to improve convergence. A 22 × 36 nonuniform grid was employed in the $\theta \times \eta$ computational domain shown in the inset of Fig. 1. Here, the grid lines were closely packed near the wall and near the fin locations. The axial steps were smaller in the vicinity of the entrance, increasing gradually in the downstream region. Solution by a marching procedure was obtained along Z until the fully developed thermal regime was reached. The computed results are accurate to at least 0.1% for the asymptotic Nusselt number.

One-Dimensional Lumped Formulation

A one-dimensional energy balance on a thermodynamic control volume yields the dimensionless lumped energy equation, along with its inlet boundary condition:

$$\frac{d\phi_b}{dZ} = 2\overline{Nu}_{eq}(1 - \phi_b), \qquad \phi_b(0) = 0 \tag{7}$$

The key parameter in this ordinary differential equation of first order is the mean, equivalent Nusselt number $\overline{Nu}_{eq} = \bar{U}D/k_i$

$$1/\overline{Nu}_{eq} = (1/\overline{Nu}_i) + (1/2Bi_{mean}) \tag{8}$$

that defines a harmonic mean of $\overline{Nu}_i(\bar{L})$ and $2Bi_{mean}$. Equation (8) is nothing more than the dimensionless version of the mean, overall heat transfer coefficient $\bar{U}$, linking the heat exchange between an internal fluid and an external fluid through a dividing wall.[2] Correspondingly, to be consistent with the physical aspects of the lumped model, the functional relations for both $\overline{Nu}_i(\bar{L})$ and Bi_{mean} must conform with an isothermal temperature at the wall T_w in the thermodynamic control volume. The numerical value of $\overline{Nu}_i(\bar{L})$ may be obtained by evaluating Hausen's correlation equation[2,3]

$$\overline{Nu}_i = \frac{\bar{h}_i D}{k_i} = 3.657 + \frac{0.134/\bar{L}}{1 + 0.064/\bar{L}^{2/3}} \tag{9}$$

where $\bar{L} = L/RPe_i$ denotes a dimensionless axial station.

The angular variation of the Biot number $Bi(\theta)$ may be recast as two separate Biot numbers, Bi_u and Bi_f, belonging to the unfinned and finned segments, X_u and X_f, respectively. Therefore, three different weighted-spatial-means of the Biot number Bi_{mean} may be constructed from statistical theory as follows:

The arithmetic-spatial-mean:

$$Bi_a = \frac{X_u Bi_u + X_f Bi_f}{X_u + X_f} \tag{10}$$

The harmonic-spatial-mean:

$$Bi_h = \left[\frac{1}{X_u + X_f}\left(\frac{X_u}{Bi_u} + \frac{X_f}{Bi_f}\right)\right]^{-1} \tag{11}$$

The geometric-spatial-mean:

$$Bi_g = (Bi_u^{X_u} Bi_f^{X_f})^{1/(X_u+X_f)} \tag{12}$$

In light of the foregoing, Eq. (7) becomes separable because $\overline{Nu}_{\text{eq}}$ is simply a number. Moreover, the simplicity of Eq. (7) gives rise to an analytical solution that can be readily evaluated by hand or a calculator:

$$\phi_b(\bar{L}) = 1 - \exp(-2\overline{Nu}_{\text{eq}}\bar{L}) \tag{13}$$

By choosing various axial stations $\bar{L}$, the bulk temperatures $\phi_b(\bar{L})$ may be computed immediately from Eq. (13) after an adequate spatial-mean Bi has been selected from the previous list.

Discussion of Results

There are four controlling parameters: 1) N, 2) X_f, 3) Bi_f, and 4) Bi_u. Owing to an abundance of parameters coupled with journal space limitations, only representative results will be given here for two arrays consisting of $N = 4$ and 16 fins. Fixed values of the parameters $X_f = 0.05$, $Bi_f = 50$, and $Bi_u = 1$ have been chosen to conduct the calculations for both arrays. For purposes of comparison, the bulk temperatures based on the three-dimensional distributed model may be regarded as the exact baseline solution. The heat transfer performance will be presented in Figs. 1 and 2 with the bulk temperature ϕ_b along the ordinate and the axial position Z along the abscissa. As expected, the total heat liberation Q_T is enhanced as the number of fins increases.

Without loss of generality, we should anticipate that the exact bulk temperatures based on the three-dimensional distributed model will lie somewhere in between those bulk temperatures calculated with the approximate one-dimensional lumped model. For the one-dimensional model, the data based on the arithmetic-spatial-mean Bi_a are portrayed by circles, whereas those for the geometric-spatial-mean Bi_g are identified by triangles. The curves that are situated in the upper part of each figure are for the one-dimensional model with Bi_a (upper bound), while those in the lower part of the figures are for the Bi_g (lower bound). The importance of the latter rests on its association with the minimum heat removal capabilities of the externally finned tube, say $Q_{T\min}$. The results for the harmonic-spatial-mean Bi_h being a weak lower bound are not plotted in the figures in order to preserve clarity.

From an overall appraisal of both figures, it is seen that none of the approximate temperature estimates are very far from those given by the exact temperature predictions. This is an affirmation of the forgiving nature of the discontinuous external convective coefficients $h_e(\theta)$, which are conveniently embedded into the dependable spatial means, h_a and h_g, respectively. The main message of these figures is revealed when overall comparisons are made among the successive set of figures. First, it may be observed that for a sparse array, $N = 4$, the bulk temperature curve supplied by the one-dimensional model with Bi_g is moderately lower than the exact bulk temperature curve based on the three-dimensional model. It may be observed that the curve of the one-dimensional model is shifted upwards, providing a qualitative statistical estimate. As the number of fins in the array is increased, an approximate symmetrical behavior is noticed and the exact curves are equidistant from the bounding curves. In contrast to the case for $N = 4$, the opposite pattern is in evidence for a dense array of 16 fins. Here, the disparity between the temperature curves of the one-dimensional model with Bi_a and the exact curve of the three-dimensional model is very small. This tendency demonstrates that the curve of the one-dimensional model is shifted downwards, supplying another qualitative statistical estimate. These features elucidated in Figs. 1 and 2 are worthy of note because they put in evidence an intrinsic sweeping behavior attached to the one-dimensional temperature curves.

References

[1]Mills, A. F., *Heat Transfer*, Irwin, Boston, MA, 1992.

[2]Hausen, H., "Darstellung des Warmeuberganges in Rohren durch verallgemeinerte Potenzbeziehungen," *Z. VDI Beih. Verfahrenstech*, No. 4, 1943, pp. 91–95.

[3]Patankar, S. V., *Numerical Heat and Fluid Flow*, Hemisphere, Washington, DC, 1980.

Self-Oscillation Enhancement of Impingement Jet Heat Transfer

R. H. Page,* P. S. Chinnock,† and J. Seyed-Yagoobi‡
Texas A&M University,
College Station, Texas 77843-3123

Introduction

IMPINGING jets are currently widely used in manufacturing and other commercial operations. In some cases it had been found that an oscillation forced on the flow improved the heat transfer, but required auxiliary external power to drive the device that caused the oscillation. Our objective was to produce enhanced heat transfer without an external power source.

Experimental and theoretical studies of transport phenomena augmentation devices that would be useful for retrofitting existing nozzles had been under way at Texas A&M University. The self-oscillating jet impingement nozzle (SOJIN) was developed under the leadership of R. H. Page. It was demonstrated by making a minor addition to a standard in-line jet impingement nozzle. A schematic of the standard in-line jet (ILJ) nozzle and the SOJIN is shown in Fig. 1. The collar is extended over the o.d. of the existing nozzle to a distance where the shear tone frequency is in resonance with the organ pipe frequency of the existing nozzle.[1–3] A self-oscillation then occurs that has been found to enhance the surface transport phenomena.

Received April 20, 1995; revision received Oct. 30, 1995; accepted for publication Oct. 30, 1995.

*Professor Emeritus of Mechanical Engineering. Associate Fellow AIAA.

†Graduate Research Assistant, Mechanical Engineering Department.

‡Associate Professor of Mechanical Engineering and Director of Drying Research Center.